Human immunodeficiency virus type-1 infection impairs the formation of the immunological synapse.

Maria Isabel Thoulouze, Nathalie Sol-Foulon, Fabien Blanchet, Alice Dautry-Varsat, Olivier Schwartz, Andrés Alcover

Immunity 24, 1–15, May 2006 ©2006 Elsevier Inc. DOI 10.1016/j.immuni.2006.02.016

Human Immunodeficiency Virus Type-1 Infection Impairs the Formation of the Immunological Synapse

Maria Isabel Thoulouze,[1,2,4,5] Nathalie Sol-Foulon,[3,5] Fabien Blanchet,[3] Alice Dautry-Varsat,[2] Olivier Schwartz,[3,6,*] and Andrés Alcover[1,2,6,*]

[1] Unité de Biologie Cellulaire des Lymphocytes
[2] Unité de Biologie des Interactions Cellulaires
Centre National de la Recherche Scientifique Unité de Recherche Associée-2582
[3] Groupe Virus et Immunité
Centre National de la Recherche Scientifique Unité de Recherche Associée-1930
Institut Pasteur
25-28, rue Dr Roux
75724 Paris Cedex 15
[4] Unité de Virologie et Immunologie Moléculaires
Institut National de la Recherche Agronomique
Jouy-en Josas
France

Summary

HIV-1-infected lymphocytes improperly respond to T cell antigen receptor (TCR) stimulation. To document this phenomenon, we studied the capacity of HIV-1-infected lymphocytes to form immunological synapses. We show here that HIV-1-infected T cells poorly conjugated with antigen-presenting cells, and when they formed conjugates, the synapses were abnormal. TCR and Lck accumulated in the recycling endosomal compartment, and their clustering at the synapse was severely reduced. These phenomena were, to a large extent, caused by Nef, a viral protein affecting intracellular trafficking and signaling pathways. Concomitantly, in HIV-infected cells, tyrosine phosphorylation at the synapse and the patterns of tyrosine phosphorylated proteins were disturbed in a Nef-dependent manner. These findings underscore the importance of Lck and TCR endosomal trafficking in synapse formation and early T cell signaling. Alteration of endocytic and signaling networks at the immunological synapse likely impacts the function and fate of HIV-1-infected cells.

Introduction

Soon after antigen recognition by T cells, TCRs, coreceptors, adhesion molecules, and signaling and cytoskeleton components accumulate and form supramolecular clusters at the T cell-APC contact site, termed the immunological synapse (Grakoui et al., 1999; Monks et al., 1998). Immunological synapses are thought to structure in time and space the complex communication between the T lymphocyte and the APC, in a way to ensure efficient antigen recognition and controlled T cell activation, and to provide stimuli to the APC.

*Correspondence: schwartz@pasteur.fr (O.S.); aalcover@pasteur.fr (A.A.)
[5] These authors contributed equally to this work as first authors;
[6] These authors contributed equally to this work as senior authors.

To concentrate at the immunological synapse, receptors and signaling molecules need to be targeted to the APC contact site and retained there. Molecular translocation may occur through lateral mobility at the plasma membrane (Wülfing and Davis, 1998), as well as via intracellular vesicular trafficking. The latter concerns surface receptors, like TCR or CTLA-4 (Das et al., 2004; Egen and Allison, 2002), as well as intracellular signaling molecules, like Lck or LAT (Bonello et al., 2003; Bunnell et al., 2002; Ehrlich et al., 2002).

HIV and SIV cause AIDS primarily by infecting $CD4^+$ T lymphocytes. Signaling pathways and transcriptional activation, as well as intracellular protein trafficking, are altered in HIV-infected cells. HIV proteins Nef and Tat may increase T cell activity, thus facilitating viral replication (Simmons et al., 2001; Wu and Marsh, 2001). Nef also affects trafficking and surface levels of several receptors, including CD4, CD28, and MHC molecules (for review, see Das and Jameel [2005], Piguet et al. [1999]). Moreover, the apoptotic signaling machinery is modulated by Nef (Geleziunas et al., 2001; Wolf et al., 2001). Viral envelope glycoproteins also impact T cell function, likely by interacting with CD4 and coreceptors. Finally, a small proportion of lymphocytes becomes latently infected quiescent cells through poorly defined mechanisms (Williams and Greene, 2005). All these observations point out to a model in which HIV-1 reshapes the host's intracellular environment so as to optimize viral propagation and cell survival.

Little is known about the consequences of HIV infection on the constitution of the immunological synapse. We show here, by using wild-type (wt) as well as *nef*-deleted HIV and either primary $CD4^+$ T cells or Jurkat lymphoid cells as targets, that infected cells are impaired at different levels in their capacity to form immunological synapses. Key phenomena, such as the conjugation of T cells with APCs and the subsequent clustering of TCR and Lck at the contact zone, were strongly inhibited. These alterations were dependent on Nef, which prevented the correct targeting of TCR and Lck to the immune synapse by altering their intracellular trafficking. Moreover, tyrosine-phosphorylation patterns were inhibited in a Nef-dependent manner.

Results

HIV-1 Infection Impairs T Cell-APC Conjugate Formation and TCR Clustering at the Immunological Synapse

Constitution of immunological synapses is associated with a coordinated reorganization of activation and vesicle trafficking pathways in lymphocytes (Bonello et al., 2003; Das et al., 2004; Egen and Allison, 2002; Ehrlich et al., 2002; Krogsgaard et al., 2003). The recycling endosomal compartment polarizes toward the T cell-APC contact site, and TCRs, as well as signaling molecules like Lck or LAT, in transit through recycling endosomes, are targeted to the synapse (Bonello et al., 2003; Das et al., 2004; Ehrlich et al., 2002). Since HIV-1 infection is associated with important alterations of intracellular

signaling and trafficking events (Greenway et al., 2003; Piguet et al., 1999), we examined how HIV-1-infected lymphocytes form immunological synapses. To this end, human Jurkat lymphoid cells, or primary $CD4^+$ lymphocytes, were infected with the HIV-1 X4-tropic strain NL4.3. Synapses formed between T cells and superantigen (sAg)-pulsed APCs (B cell lymphoma Raji) were then studied by immunofluorescence, confocal microscopy, and quantitative image analysis, as previously described (Das et al., 2004; Roumier et al., 2001).

Experiments were performed at day 3 or 4 postinfection (p.i.), before the peak of viral production and the occurrence of major virus-induced cytopathic effects. Cell viability was assessed by controlling scatter profiles and apoptotic markers by flow cytometry (see Figure S1 in the Supplemental Data available with this article online). About 30%–60% of Jurkat cells and 20%–40% of PBLs were productively infected, as judged by intracellular Gag staining.

Strikingly, the percentage of cell conjugates formed between HIV-1-infected (or Gag^+) lymphocytes and sAg-pulsed APCs was about 3-fold lower than that in noninfected cells (20% versus 60%, respectively). Similar results were obtained with Jurkat cells and with PBLs, and at a later time point (30 min, data not shown), indicating that HIV-infected lymphocytes poorly interact with APCs (Figure 1A).

We then assessed the accumulation of TCRs at the T cell-APC contact site, a hallmark of the immunological synapse (Grakoui et al., 1999; Monks et al., 1998). In the absence of APCs, TCR-CD3 surface levels were similar or slightly higher in infected cells than in controls, whereas CD4 and, CD28 were, as expected, downregulated (Figure S2). Confocal microscopy showed that, in the absence of sAg, TCR molecules were randomly distributed at the cell surface (Figures 1B, 1C, 1F, and 1G). Moreover, as expected, when control cells were incubated with sAg-pulsed APCs, TCR clusters were readily detected in the T cell-APC contact zone (Figures 1D and 1H; arrows). In contrast, in Gag^+ cells, TCR clusters appeared more punctate and less intense (Figures 1E and 1I, arrows). Quantitative analysis of the fluorescence intensity of these clusters showed a 5- to 6-fold lower signal in conjugates formed by infected cells, in both Jurkat and PBLs, at 15 or 30 min of activation (Figures 1J and 1K). Of note, similar experiments were performed at day 1 p.i. The fraction of infected cells was low at this time point, but synapses formed by Gag^+ cells also displayed diminished TCR accumulation (data not shown). Altogether, these data show that HIV-1-infected lymphocytes incorrectly form immunological synapses.

HIV-1 Infection Inhibits Lck Targeting to the Immunological Synapse

Conjugate formation between T cells and APCs and TCR clustering at the immunological synapse are regulated by TCR signaling (Huppa et al., 2003; Kinashi, 2005). Lck is the first tyrosine kinase activated after TCR engagement. Its activity promotes inside-out signaling to integrins, necessary for T cell-APC adhesion (Morgan et al., 2001), and induces actin cytoskeleton remodeling needed for TCR clustering (Sechi and Wehland, 2004). Lck is localized at the plasma membrane and in an intracellular pericentriolar compartment that overlaps with early endosomes (Ehrlich et al., 2002; Ley et al., 1994). Upon antigen recognition, Lck from membrane and vesicular pools translocates to the APC contact site, where it becomes transiently activated (Ehrlich et al., 2002; Lee et al., 2002). We hypothesized that HIV-1 infection could impair Lck targeting to the synapse and, as a consequence, inhibit T cell-APC conjugate stability and TCR clustering. We therefore investigated the impact of HIV-1 on the subcellular localization of Lck.

As expected, uninfected cells displayed Lck at the cell cortex and, to a minor extent, in an intracellular vesicular compartment, more visible in Jurkat than in PBLs (Figures 2A and 2E, arrowhead). In HIV-1-infected cells, the amount of vesicular Lck was strongly increased, whereas the cortical signal became very faint. This occurred in both Jurkat and PBLs, independently of sAg stimulation, or T cell-APC contact (Figures 2B and 2F; arrowheads). When infected lymphocytes were incubated with sAg-pulsed APCs, the endosomal pool of Lck polarized toward the APC contact site (Figures 2D and 2H; arrowheads). However, the amount of Lck clustered at the synapse was severely reduced (Figures 2D and 2H versus Figures 2C and 2G; arrows). Image quantification showed that, in unstimulated T cells, the amount of endosomal Lck was about 5-fold higher in HIV-1-infected than in control cells. Conversely, the amount of Lck accumulated at the synapse was about 6-fold lower in infected cells (Figures 2I and 2J).

Lck traffics through transferrin $(Tf)^+$ endosomes (Ehrlich et al., 2002). We therefore asked whether Lck accumulates in these endosomes in infected cells. Since various vesicular compartments concentrate in the pericentriolar area, we increased image resolution by carrying out deconvolution and 3D reconstruction, and we quantified Lck and Tf receptor (TfR) colocalization (displayed as dot plot diagrams). In control cells, Lck was in close proximity to TfR but only weakly colocalized with it (few dots in the diagonal on the colocalization plot, Figure 2K and Movie S1). In contrast, in infected cells, a stronger colocalization was observed in the central area of the TfR^+ compartment (numerous dots appear in the diagonal of the plot, Figure 2L and Movie S2). This indicates that HIV-1 perturbs Lck and TfR trafficking, which mix together in some subregions of the endosomal compartment.

Altogether, these results indicate that HIV-1 infection inhibits Lck targeting to the immunological synapse by retaining this kinase in the recycling endosomal compartment.

HIV-1 Nef Promotes Lck Retention in the Endosomal Compartment

Among HIV proteins, Nef is known to interfere with the cellular sorting machinery, modulating the expression of various receptors (for review, see Das and Jameel [2005], Piguet et al. [1999]). We thus investigated the impact of Nef on Lck trafficking and immune synapse formation. Jurkat or PBLs were infected with wt, or Nef-defective virus (HIVΔ*nef*) with an moi enough to obtain a similar fraction of productively infected cells (about 60%–30% of Jurkat cells and 30%–15% of PBLs were infected with wt and Δ*nef* virus, respectively). Experiments were performed 3 or 4 days p.i., without any

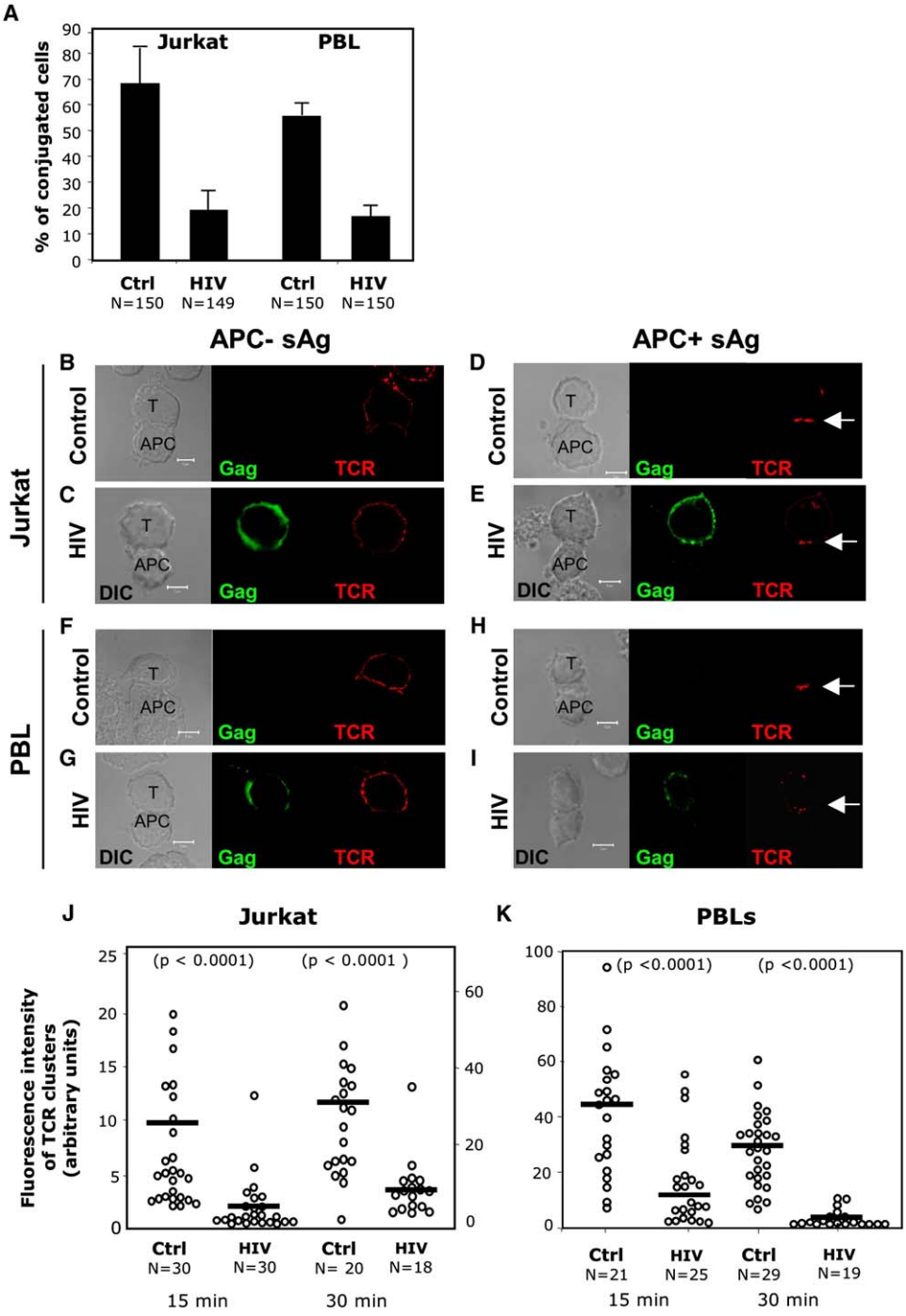

Figure 1. HIV-1 Infection Impairs T Cell-APC Conjugate Formation and TCR Clustering at the Immunological Synapse

Jurkat, or sAg-specific PBLs, were infected with HIV-1. Three to four days p.i., infected (HIV) or noninfected T cells (control) were incubated for 15 or 30 min with APC (Raji) pulsed with medium alone or with sAg. Cells were fixed and stained with anti-CD3 mAb under nonpermeabilizing conditions to detect only surface TCRs. Cells were then permeabilized and stained with anti-Gag Ab in order to detect infected cells. DIC, differential interference contrast image. Scale bar, 5 μm. (A) T cell-APC conjugates formed during 15 min between noninfected or infected T cells and sAg-pulsed APCs were scored by visual counting under a fluorescence microscope. Infected cells were assessed by Gag staining. (B–I) T cell-APC conjugates formed during 15 min in the absence or in the presence of sAg analyzed by confocal microscopy. Images show a medial optical section of a representative cell. Arrows point to TCR clusters. (J and K) Quantitative image analysis of TCR accumulation at the immunological synapse performed as described in methods. Each dot represents a T cell-APC conjugate. The bar shows the mean value. The statistical analysis p values between adjacent plots are shown in brackets.

obvious virus-induced cytopathic effect (Figure S1). As expected, HIVΔ*nef* lost its capacity to downregulate the surface expression of CD28. CD4 was downregulated, although to a lesser extent, in Δnef-infected cells, likely by other viral proteins (Env and Vpu) known to act on this receptor (Figure S2).

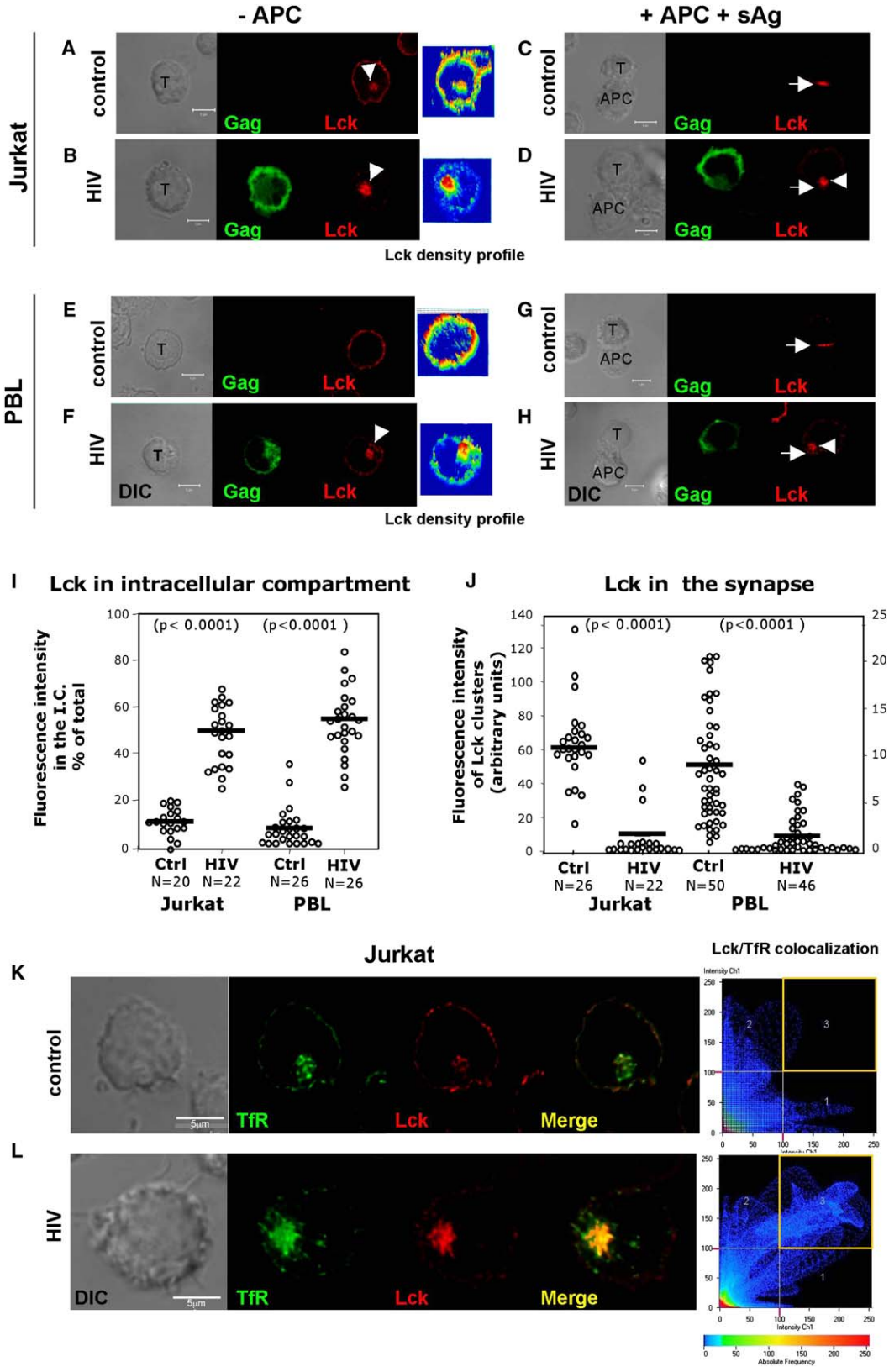

Figure 2. HIV-1 Infection Induces the Accumulation of Lck in Endosomes and Inhibits Lck Clustering at the Immunological Synapse

Jurkat cells or sAg-specific PBLs were left uninfected or infected with HIV-1. Three to four days p.i., infected (HIV) or noninfected (control) T cells were left alone or incubated for 15 min with sAg-pulsed APC (Raji) and fixed and stained with anti-Lck and anti-Gag or with anti-Lck and anti-TfR. Scale bar, 5 μm. (A, B, E, and F) Subcellular distribution of Lck displayed by T cells. A single medial optical section is shown in the fluorescence picture. Arrowheads point to Lck in the intracellular compartment. Right panels represent the density profiles of Lck fluorescence obtained from

Interestingly, lymphocytes infected with HIVΔ*nef* formed conjugates with sAg-pulsed APCs more efficiently than HIVwt-infected cells, although without reaching the levels of controls (Figure 3A). Therefore, Nef is involved in this inhibition, and, besides Nef, other viral components might affect T cell-APC conjugate formation.

We then examined the intracellular localization of Lck. In sharp contrast with HIVwt, significant endosomal retention of Lck was observed with HIVΔ*nef* neither in Jurkat nor in PBLs (Figures 3C and 3G). Moreover, HIVΔ*nef*-infected lymphocytes efficiently clustered Lck at the synapse (Figures 3E and 3I; arrows). Image quantification shows that HIVΔ*nef*-infected cells behave like uninfected cells regarding the presence of Lck in the intracellular compartment, but they appeared mildly affected with regard to Lck clustering in the synapse (Figures 3J and 3K).

Previous studies reported an interaction between Nef and Lck (Baur et al., 1997; Collette et al., 1996). Therefore, we analyzed the localization of these proteins in infected cells. Nef was found throughout the cell cytoplasm in a tubulovesicular compartment, which colocalized with Lck in the pericentriolar region. (Figure 3L). This suggests that the interaction of Nef with Lck may be involved in the endosomal retention of Lck.

We then asked whether Nef by itself was sufficient to perturb Lck localization and immune synapse formation. Jurkat cells were transduced with lentiviral vectors expressing wild-type Nef (Nef-wt), or an inactive myristoylation-defective mutant (Nef-G2A), which no longer associates with cellular membranes (Sol-Foulon et al., 2004). About 90% of transduced cells expressed Nef, as judged by immunofluorescence staining (data not shown). Importantly, the capacity of Nef-wt-expressing lymphocytes to form conjugates with sAg-pulsed APCs was impaired, whereas cells expressing Nef-G2A were normal (Figure 4A). Moreover, Nef-wt, but not Nef-G2A, induced endosomal retention of Lck (Figure 4B; arrowhead) and reduced clustering at the synapse (Figure 4E; arrows). As in HIV-1-infected cells, Nef-wt was localized at the cell cortex and in the pericentriolar area (Figures 4B and 4E; arrowheads), whereas Nef-G2A displayed a more diffuse staining throughout the cell (Figures 4C and 4F). The proportion of endosomal Lck in Nef-wt$^+$ cells was about 5-fold higher than in control or in Nef-G2A$^+$ cells. Consistently, Lck clustering at the synapse was reduced by about 3-fold with Nef-wt, but not with Nef-G2A (Figures 4H and 4I). Finally, as in HIV-1-infected cells, Nef and Lck colocalized in the pericentriolar compartment (Figure 4J). This indicates that Nef is sufficient to impair Lck intracellular trafficking and immune synapse formation.

HIV-1 Nef Alters TCR Endocytic Trafficking

Inhibition of TCR accumulation at the synapse in HIV-1-infected cells (Figure 1) could be the consequence of impaired signaling due to Lck mislocalization. In addition, HIV-1 infection could alter TCR endocytic trafficking, which is necessary for its targeting to the synapse (Das et al., 2004). Therefore, we analyzed the subcellular localization of TCR. In the experiments presented in Figure 1, staining was performed on nonpermeabilized cells in order to visualize only TCRs expressed at the cell surface. We next conducted experiments on permeabilibized cells, to get a complete view of TCR localization. In control cells, intracellular TCR staining gave a diffuse and vesicular cytoplasmic pattern (Niedergang et al., 1995), which is due to the presence of TCR-CD3 subunits in the endoplasmic reticulum as well as in endosomes (Figure 5A). In HIV-1-infected cells, a more prominent TCR$^+$ pericentriolar vesicular compartment was detected, which was easily visible in fluorescence density profiles (Figure 5B; right blue panel). TCR staining overlapped with that of TfR, indicating that TCR accumulates in recycling endosomes in infected cells.

TCR intracellular accumulation was also detected in cells expressing Nef-wt alone (Figure 5F), but not in HIVΔ*nef*-infected cells (Figure 5C) or in Nef-G2A-expressing cells (Figure 5G). Conversely, Nef-wt, but not Nef-G2A, decreased TCR accumulation at the synapse (Figures 5I and 5J). The presence of TCR in the pericentriolar compartment was about 2- to 3-fold higher in cells infected with HIV-1-wt, or in cells expressing Nef alone (Figures 5D and 5H). Conversely, TCR clustering at the synapse was about 2-fold lower in cells expressing Nef-wt than in control cells or in those expressing Nef-G2A (Figure 5K).

We then measured the kinetics of TCR endocytic trafficking. The phorbol ester PdBu induces TCR internalization and reversible accumulation in recycling endosomes (Niedergang et al., 1997). This mimics TCR constitutive endocytosis and recycling, since it depends on the phosphoserine-dependent dileucine motif of the CD3γ subunit (Dietrich et al., 2002). TCR endocytosis and further recycling can be measured by flow cytometry following downregulation of surface TCR-CD3 upon PdBu addition and further reexpression after PdBu wash.

We compared TCR dynamics in control, HIV-1 wt-, and Δ*nef*-infected Jurkat cells. Costaining of Gag was used to detect infected cells. Cells were pretreated with cycloheximide in order to suppress protein synthesis. Steady-state surface staining of cells without PdBu defined 100% levels for each cell type. In control cells, as well as in cells infected with HIVΔ*nef*, a rapid TCR internalization was observed upon PdBu addition, with 40%–50%

a XY projection of five medial optical sections. Color scale goes from blue (zero) to yellow (intermediate) to red (maximal). (C, D, G, and H) Subcellular distribution of Lck displayed by T cell-APC conjugates at 15 min of activation. Arrowheads point to Lck accumulated in the intracellular compartment, whereas arrows point to Lck clusters at the immunological synapse. (I and J) Quantitative image analyses of Lck accumulation in the intracellular compartment (I.C.). Plots show the percentage of fluorescence intensity in the intracellular compartment with respect to the total cell fluorescence, or the total fluorescence per Lck cluster, respectively. Each dot represents an isolated T cell or a T cell-APC conjugate. The bar shows the mean value. The statistical analysis p values between adjacent plots are shown in brackets. (K and L) Subcellular localization of Lck and TfR in control or HIV-1-infected Jurkat cells. Confocal images posttreated by deconvolution are shown. Medial optical sections where colocalization was maximal are shown. Right panels show colocalization diagrams of the same section. Dots in the diagonal represent pixels where colocalization of both types of fluorescence occurs. Pixels displaying colocalization (upper right squares) are depicted in yellow in the merge image. 3D reconstructions of these images are shown in Movies S1 and S2.

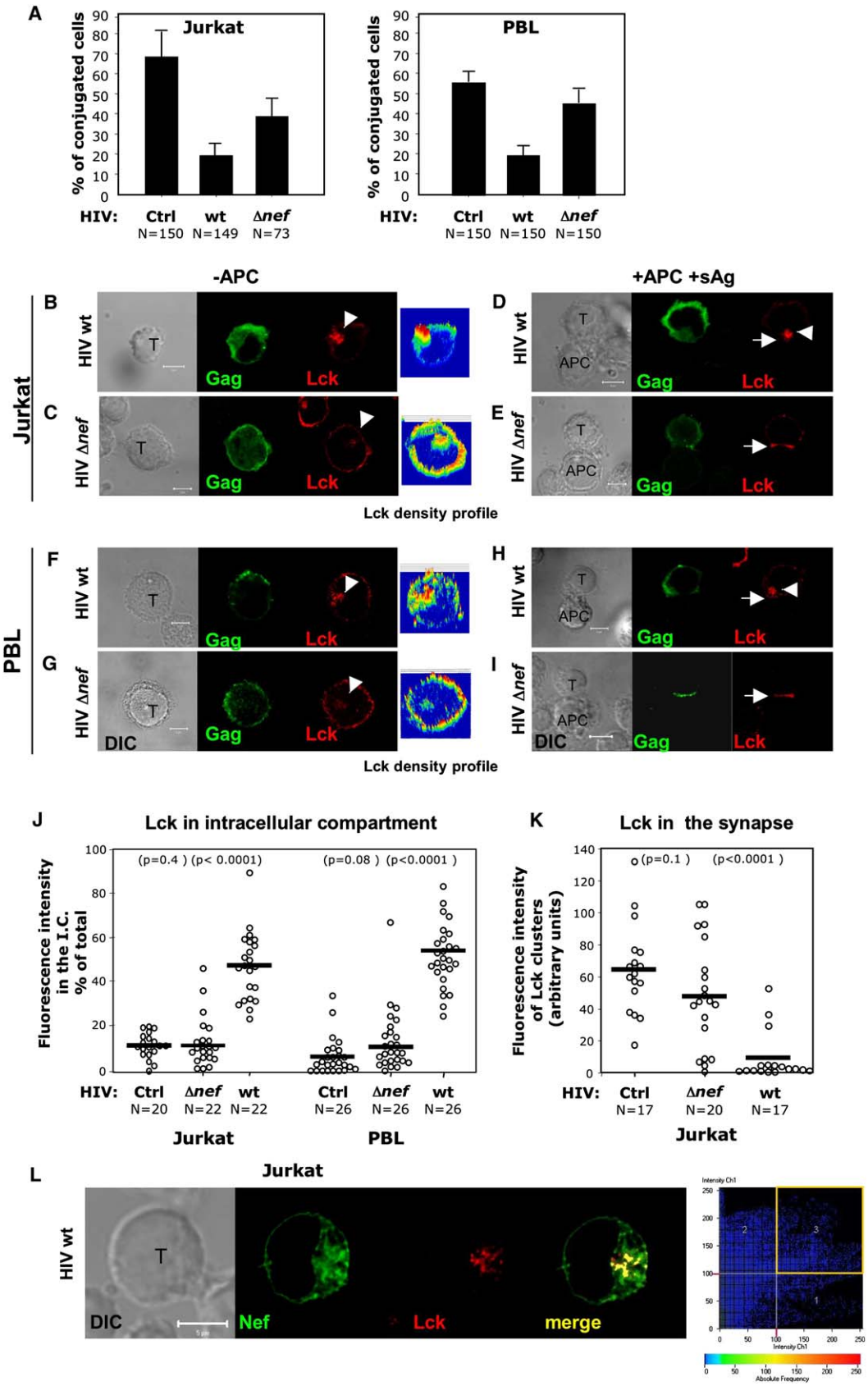

Figure 3. HIV-1 Nef Is Involved in Lck Accumulation in the Endosomal Compartment

Jurkat cells or sAg-specific PBLs were left uninfected (control), or they were infected with HIV-1 wt or Δ*nef*. Three to four days p.i., T cells were left alone or incubated for 15 min with sAg-pulsed APC and fixed and stained using anti-Lck mAb and anti-Gag Ab or anti-Lck and anti-Nef mAbs.

of surface molecules disappearing in 30 min. PdBu removal induced the reexpression of internalized molecules reaching 80% of surface expression, after an additional 60 min. In contrast, in cells infected with HIV-wt, TCR internalization was impaired, and 90% of TCRs remained at the cell surface after 30 min of PdBu treatment. Moreover, a less efficient TCR re-expression was observed upon PdBu wash. In contrast, Δ*nef* virus did not significantly delay TCR internalization, although reexpression was slightly affected (Figure 5L).

Nef was shown to change the morphology of the endosomal compartment and to reduce Tf recycling (Madrid et al., 2005; Sanfridson et al., 1997). This could account for the alterations in Lck and TCR trafficking reported here. Therefore, we assessed whether TfR trafficking was altered in infected cells. TfR surface levels were reduced in HIV-1-infected Jurkat cells (Figure S3), whereas the amount of pericentriolar TfR was increased (data not shown). Thus, trafficking through the endosomal recycling compartment seems to be inhibited in infected cells and affects molecules like Lck, TCR, and TfR. However, the Nef effect was different, Lck and TfR appear mainly impaired at the recycling step (Figures 2 and 3) (Madrid et al., 2005), whereas TCR trafficking is delayed mainly at the endocytosis and, to a lesser extent, at the recycling step (Figure 5L). Consistently, surface levels of TfR are reduced, whereas those of TCR are unaffected or slightly increased in infected cells (Figure S3). Of note, the levels of other molecules, such as ICAM-3, LFA-1 (CD11a/CD18), or CD2, remain normal (Figure S3), indicating that Nef impacts only certain T cell surface molecules.

Altogether, these data indicate that HIV-1 infection affects TCR endocytic trafficking in a Nef-dependent manner. Internalization is more affected than recycling, TCRs accumulate in the endocytic compartment, and their targeting to the immunological synapse is reduced.

The Effects of HIV-1 on Lck Localization and Immune Synapse Formation Are Independent on Nef-Induced CD4 and CD28 Downregulation

Since immune synapse formation depends on the interactions of CD4 and CD28 with their ligands on the APC (Holdorf et al., 2002; Irvine et al., 2002; Krummel et al., 2000; Li et al., 2004; Vidal et al., 1999), the downregulating activity of Nef on CD4 and CD28, and its ability to disrupt Lck-CD4 interaction (Piguet et al., 1999; Salghetti et al., 1995), could inhibit immune synapse formation. To investigate this, we first asked whether the effects of Nef on Lck traffic were dependent on CD4. We studied Lck localization in a subclone of Jurkat cells, which expresses undetectable levels of surface CD4. In these cells, Nef, but not Nef-G2A, still induced endosomal accumulation of Lck (Figures S4B and S4C), indicating that this mislocalization is not the consequence of Nef-induced CD4 downregulation.

We then examined whether the effects of HIV-1 on immune synapse formation were a consequence of Nef-induced CD4 and CD28 downregulation. To this end, we studied the effect of an HIV-1 derivative carrying a NefLL/AA mutant. This NefLL/AA mutant no longer downregulates CD4 or CD28, but retains its ability to modulate MHC-I and to affect signal transduction pathways (Figure S5) (Craig et al., 1998; Das and Jameel, 2005). Since this Nef mutant was derived from the *nef* gene of the HIV SF2 strain, for comparison we used HIV-wt expressing the SF2 Nef protein. Interestingly, under infection conditions in which no CD4 or CD28 downregulation occurred (Figure S5), HIV-NefLL/AA induced Lck endosomal accumulation and abnormal TCR clustering similarly to HIV-wt (Figure 6). Moreover, HIV-NefLL/AA inhibited TCR internalization in response to PdBu as efficiently as HIV-wt (Figure 6I). Thus, mislocalization of Lck and impairment of immune synapse formation are not the consequence of Nef-induced CD4 and CD28 downregulation. Moreover, Nef proteins from different HIV-1 strains, NL4.3 and SF2, altered Lck trafficking and TCR clustering at the synapse.

HIV-1 Infection Inhibits Early Signaling Events

Lck activation is a rapid process, which begins before "mature" immunological synapses are fully formed (Lee et al., 2003). The reduced levels of Lck and TCR observed at the synapse of HIV-1 infected cells prompted us to investigate whether early signaling events were affected. To this end, we analyzed the recruitment of tyrosine-phosphorylated proteins at the synapse, a phenomenon observed within minutes of contact with APCs. This recruitment was readily visible in uninfected PBLs as well as in cells infected with HIVΔ*nef* (Figures 7A and 7C). In contrast, in HIVwt-infected cells, the posphotyrosine signal was dispersed and 3-fold less intense (Figures 7B and 7G). Consistently, cells expressing only Nefwt, but not the mutant NefG2A, displayed a significant lower accumulation of phosphotyrosine at the synapse (Figures 7D–7F and 7H). Thus, HIV-1 infection inhibits early signaling at the immune synapse in a Nef-dependent manner.

We also followed tyrosine-phosphorylated proteins by Western blot analysis (Figure 7I). After 2 min of contact with APCs, various phosphoproteins were induced and remained detectable at 15 min. From their apparent molecular masses, the phosphorylated proteins likely correspond to Vav, ZAP70, Lck, and LAT. Consistent with results obtained by immunofluorescence, the intensity of the main tyrosine phosphorylated bands observed at 2 and 15 min activation was reduced in HIV-1-infected lymphocytes when compared to uninfected or HIVΔ*nef*-infected cells. Nevertheless, HIVΔ*nef*-infected cells

(A) T cell-APC conjugates formed during 15 min were scored by visual counting under a fluorescence microscope. Cell infection was assessed by Gag staining. (B, C, F, and G) Subcellular distribution of Lck displayed by T cells. A single medial optical section is shown in the fluorescence picture. Arrowheads point to Lck in the intracellular compartment. Right panels represent the density profiles of Lck fluorescence obtained as in Figure 2. (D, E, H, and I) Subcellular distribution of Lck displayed by T cell-APC conjugates at 15 min of activation. Similar patterns were observed at 30 min (data not shown). Arrowheads point to Lck in the intracellular compartment, whereas arrows point to Lck clusters at the immunological synapse. (J and K) Quantitative image analyses of Lck accumulation in the intracellular compartment (I.C.) or in the synapse, performed as in Figure 2. Statistical p values between adjacent plots are shown in brackets. Differences between control and Δ*nef* infected cells were not significant ($p > 0.05$). (L) Subcellular localization of Lck and Nef in control or HIV-1-infected Jurkat cells. Confocal images posttreated by deconvolution were analyzed as in Figures 2K and 2L.

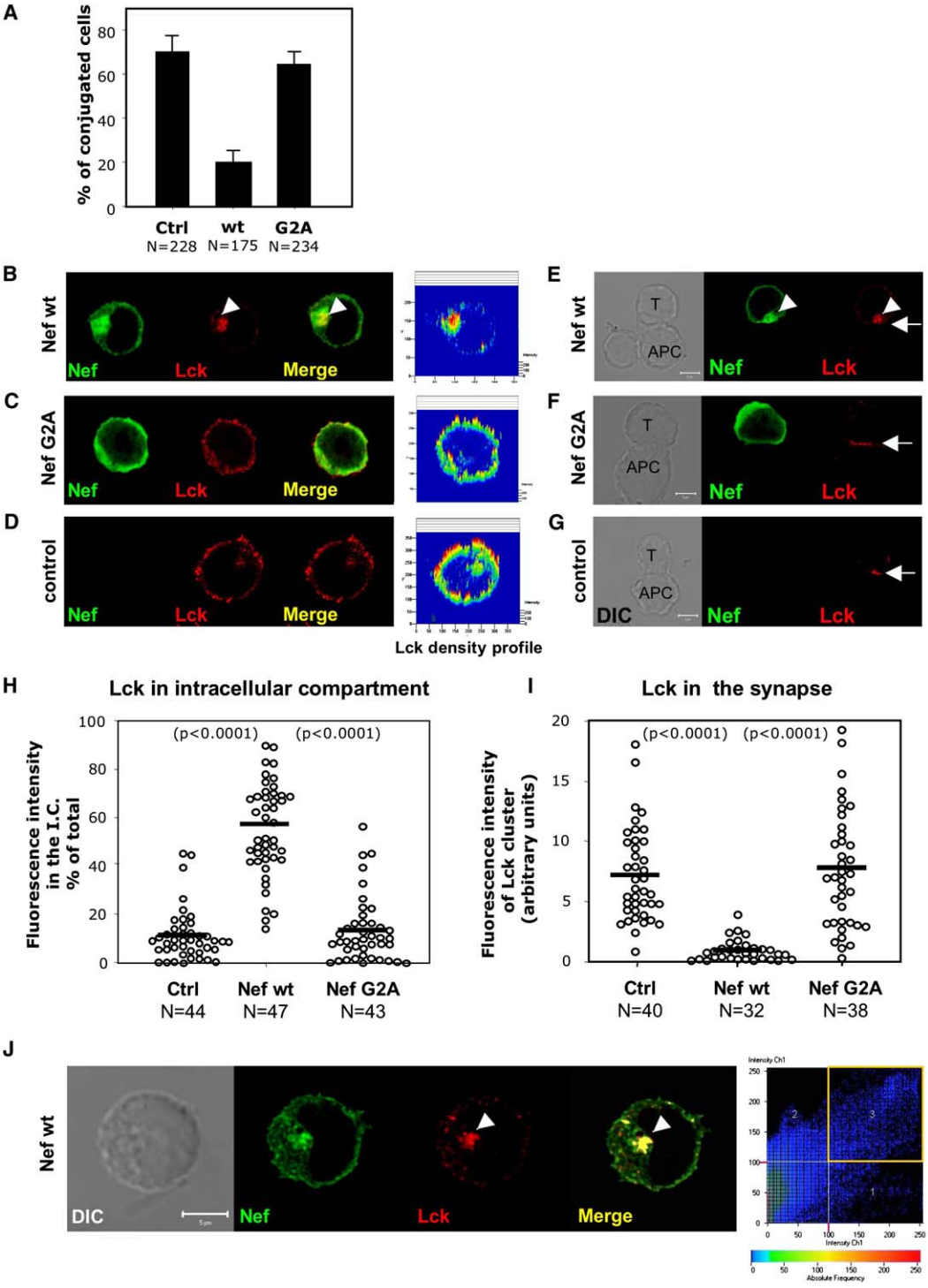

Figure 4. HIV-1 Nef Expression Is Sufficient to Induce Lck Accumulation in Endosomes and to Impair Lck Clustering at the Immune Synapse

Jurkat cells were either left nontransduced (control) or transduced with lentiviral expression vectors encoding Nef-wt or the Nef-G2A mutant. T cells were left alone or incubated for 15 min with sAg-pulsed APC and fixed and stained as in Figure 2 using anti-Nef and anti-Lck primary Abs. (A) T cell-APC conjugates formed during 15 min were scored by visual counting under a fluorescence microscope. Nef expression was assessed by anti-Nef staining. (B–D) Subcellular distribution of Lck and Nef in T cells. A single medial optical section is shown in the fluorescence picture. Arrowheads point to Lck accumulated in intracellular compartment. Right panels represent the density profiles of Lck fluorescence obtained as in Figures 2 and 3. (E–G) Subcellular distribution of Lck displayed by T cell-APC conjugates at 15 min of activation. Similar patterns were observed at 30 min (data not shown). Arrowheads point to Lck in the intracellular compartment, whereas arrows point to Lck clusters at the immunological synapse. (H and I) Quantitative image analyses of Lck accumulation in the intracellular compartment, or in the synapse, performed as in Figures 2 and 3. Statistical p values between adjacent plots are shown in brackets. Differences between control and Nef-G2A$^+$ cells were not significant ($p > 0.05$). (J) Subcellular localization of Lck and Nef in control or Nef-transduced Jurkat cells. Confocal images posttreated by deconvolution were analyzed as in Figures 2K and 2L.

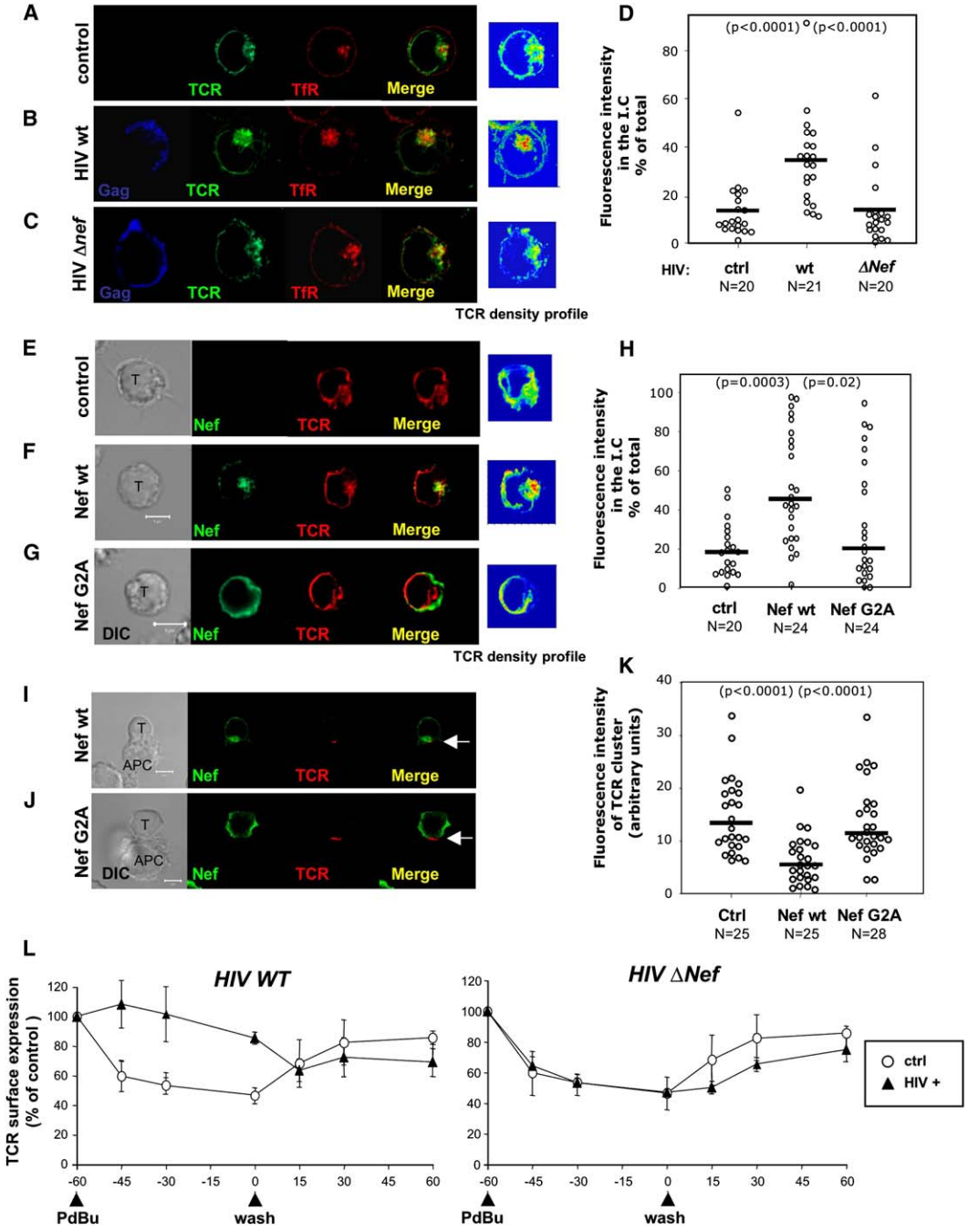

Figure 5. HIV-1 Infection Impairs TCR Intracellular Trafficking toward the Immunological Synapse

Jurkat cells were left uninfected (Ctrl), were infected with HIV-1 wt or Δ*nef* (B–D), or were transduced with lentiviral expression vectors encoding Nef-wt or Nef-G2A (F–K). At 3–4 days p.i., T cells were left alone or incubated for 15 min with sAg-pulsed APC. Cells were then fixed, permeabilized, and stained with anti-CD3, anti-TfR, and anti-Gag Abs (A–G) to reveal both intracellular and surface molecules. In (I) and (J), cells were first stained with anti-CD3, under nonpermeabilizing conditions, to reveal surface TCRs only, followed by intracellular Nef staining under permeabilizing conditions. Scale bar, 5 μm. (A–C) Subcellular distribution of TCR and TfR in T cells. A single medial optical section is shown in the fluorescence picture. Right panels represent the density profiles of TCR fluorescence obtained as in Figure 2. (E–G) Subcellular distribution of TCR and Nef in T cells. A single medial optical section is shown in the fluorescence picture. T cells had been transduced with vectors encoding Nef-wt or Nef-G2A (F and G). Right panels represent the density profiles of Lck fluorescence obtained from a XY projection of ten medial optical sections as in Figure 2. (I and J) Distribution of surface TCR and intracellular Nef in T cell-APC conjugates at 15 min activation. T cells had been transduced with vectors encoding Nef-wt or Nef-G2A. Arrows point to TCR clusters at the immune synapse. (D, H, and K) Quantitative image analyses of TCR accumulation in the intracellular compartment, or in the synapse, performed as in Figures 2–4. Statistical p values between adjacent plots are shown in brackets. Differences between control cells and cells infected with Δ*nef* or expressing Nef-G2A were not significant ($p > 0.05$). (L) Jurkat cells left unifected (ctrl), or infected with or HIV-1 wt or Δ*nef*, were incubated with the phorbol ester PdBu (1 μM) for the indicated times at 37°C. Cells were then washed (t = 0) to remove PdBu and incubated again for the indicated times at 37°C. At each time point, TCR surface expression and intracellular expression of Gag were analyzed by flow cytometry. Results are expressed as percentage of TCRs expressed at the cell surface at each time of PdBu incubation, with respect to untreated cells. Analysis was performed by gating on HIV Gag$^+$ cells.

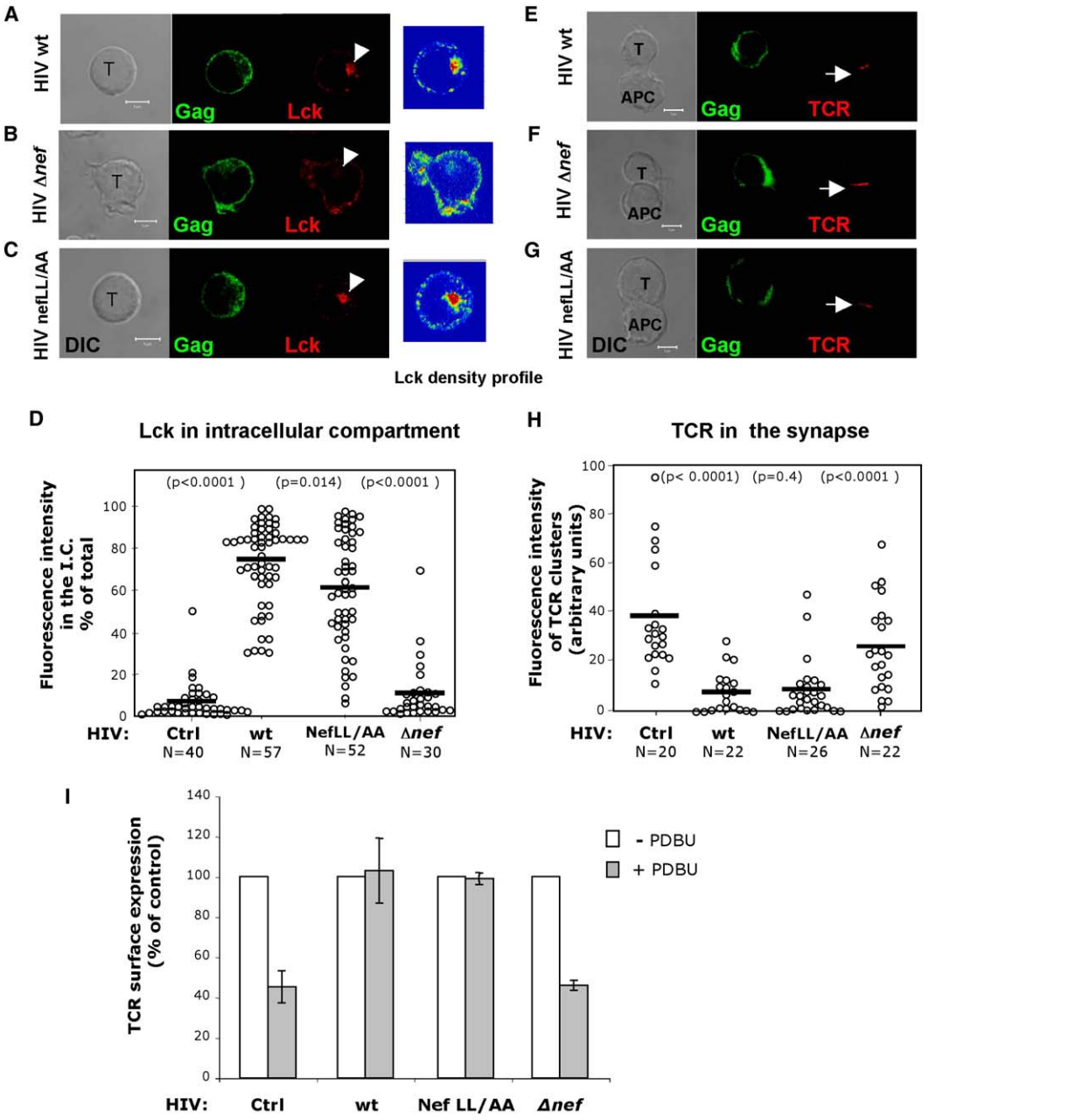

Figure 6. Lck Retention and Inhibition of TCR Clustering at the Synapse Are Independent of CD4 Downregulation

Jurkat cells were left uninfected (Ctrl), infected with HIV-1 expressing the Nef-wt, or Nef mutated in the LL motif (LL/AA), both from the SF2 virus strain. At 3–4 days p.i., T cells were left alone or incubated for 15 min with sAg-pulsed APC and fixed and stained with anti-Lck and anti-Gag. In (E)–(G), cells were first stained with anti-CD3, under nonpermeabilizing conditions, to reveal surface TCRs only, followed by permeabilization and Gag staining. Scale bar, 5 μm. (A–C) Subcellular distribution of Lck in T cells. A single medial optical section is shown in the fluorescence picture. Arrowheads point to the intracellular Lck compartment. Right panels represent the density profiles of Lck fluorescence obtained as in Figure 2. (E–G) Surface TCR distribution in T cell-APC conjugates formed after 15 min activation. A single medial optical section is shown. Arrows point to TCR clusters at the immune synapse. (D and H) Quantitative image analyses of Lck or TCR accumulation in the intracellular compartment, or in the synapse, respectively, performed as in Figures 1–5. Statistical p values between adjacent plots are shown in brackets. (I) Control or HIV-1-infected Jurkat cells were incubated with 1 μM PdBu phorbol ester for 30 min at 37°C. Cells were diluted in cold PBS, and TCR surface expression and intracellular Gag were analyzed by flow cytometry. Results are expressed as percentage of TCRs expressed at the cell surface of treated versus untreated cells. Analysis of infected cells was done by gating on Gag^+ cells.

displayed slightly impaired activation capacity (Figure 7I), suggesting that other viral proteins might also affect this process. Analysis of proteins that coimmunoprecipitated with Lck showed that the constitution of the signaling complex between Lck and downstream tyrosine-phosphorylated effectors was altered by HIVwt and, to a lower extent, by HIVΔ*nef* (Figure 7J).

Altogether, these data indicate that the effects of HIV-1 on immune synapse formation were associated with defective early T cell signaling.

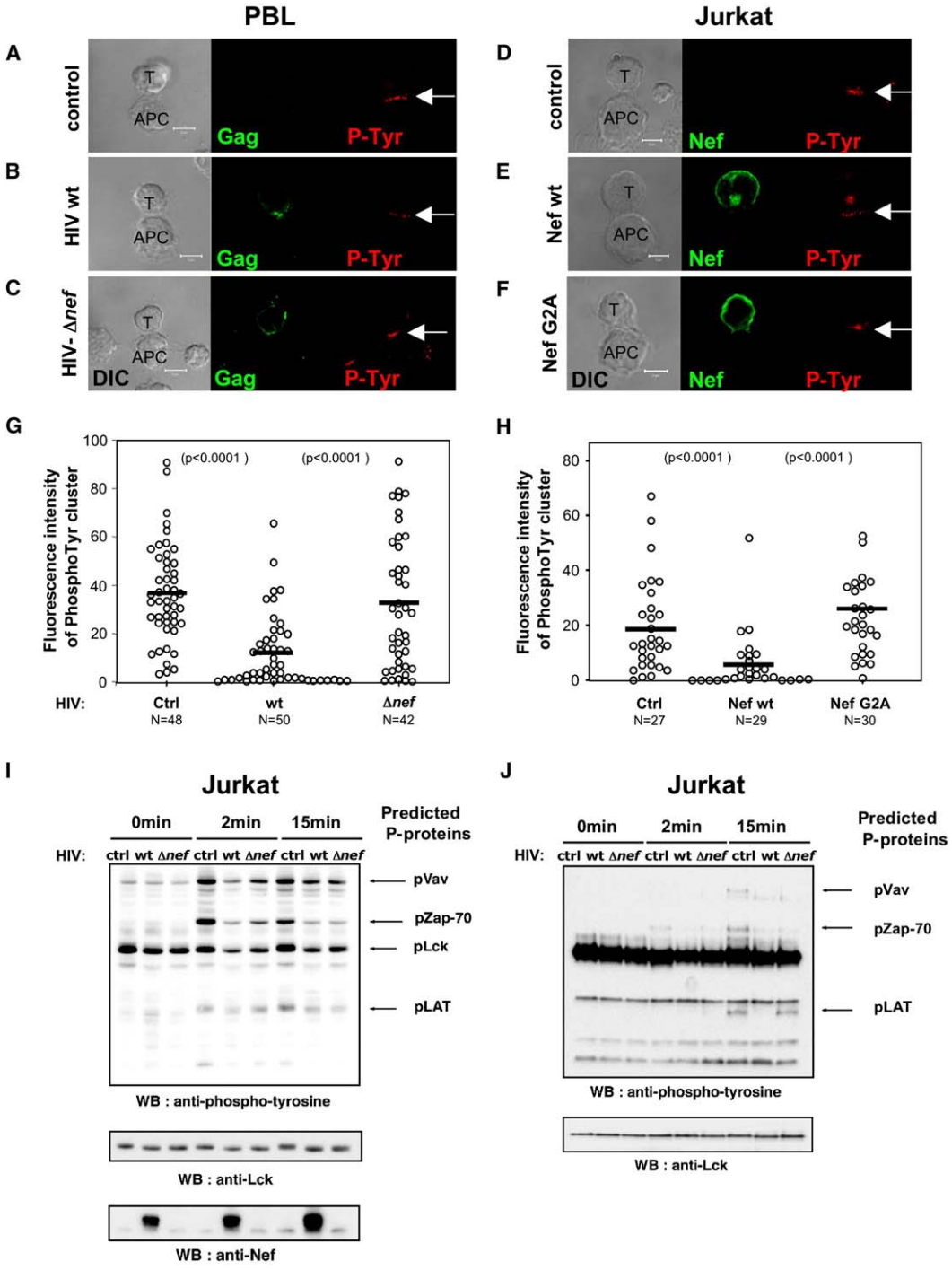

Figure 7. HIV-1 Infection Inhibits Early Signaling Events

(A–C) sAg-specific PBLs were left uninfected (control) or infected with HIV-1 wt or Δ*nef*. Three days p.i., T cells were incubated for 5 min with sAg-pulsed APC, fixed, and permeabilized and stained with anti-phosphotyrosine and anti-Gag Abs. A medial optical section of a representative cell is shown. Scale bar, 5 μm. (D–F) Jurkat cells were left untransduced or were transduced with lentiviral vectors encoding Nef-wt or Nef-G2A. Three days p.i., T cells were incubated for 5 min with sAg-pulsed APC and fixed and stained as in (A)–(C). (G and H) Quantitative image analyses of phosphotyrosine accumulation at the immunological synapse were performed as in previous figures. Statistical p values between adjacent plots are shown in brackets. Differences between control cells and cells infected with Δ*nef* or expressing Nef-G2A were not significant ($p > 0.05$). (I) Jurkat cells were left uninfected or were infected with HIV-1 wt or Δ*nef* and used at the peak of infection, as assessed by Gag staining. T cells were incubated with sAg-pulsed APCs during 2 or 5 min and lysed. Postnuclear supernatants (15×10^4 cell equivalents per lane) were analyzed by electrophoresis and Western blotting using anti-phosphotyrosine (top panel), anti-Lck (medium panel), and anti-Nef (lower panel) Abs. The predicted major phospho-proteins are indicated on the right. (J) The same lysates as in (I) (3×10^6 cell equivalents per lane) were immunoprecipitated with anti-Lck Ab and analyzed by Western blotting using anti-phosphotyrosine mAb (top) and anti-Lck Ab (lower panel). Time 0 corresponds to the mix of T cell and Raji lysates. Results are representative of four independent experiments.

HIV-1 Infection Enhances the Capacity of T Cells to Produce IL-2

Strong defects in synapse formation and reduced early T cell signaling would be expected to lead to impaired cytokine production. Therefore, we monitored IL-2 production by infected cells, upon stimulation with APCs, or with PMA and Ca-ionophore (PMA/I), which bypass TCR stimulation and immune synapse formation. Uninfected Jurkat cells did not spontaneously produce IL-2. In the presence of PMA/I, about 15% of cells produced IL-2, after 4 hr treatment. Activation through the TCR was less intense and depended on the dose of sAg, reaching 2%–3% of IL-2-positive cells. Interestingly, HIV-1 infection significantly increased IL-2 production (2- to 4-fold) with both stimuli. In the presence of APCs, this increase was even more marked with Δ*nef* than with wt virus (Figure S6) (F.B., unpublished data). In contrast, HIVwt and Δ*nef* similarly enhanced IL-2 production in response to PMA/I.

Therefore, HIV-1 likely increases IL-2 production by acting on events downstream of PKC signaling. Viral proteins capable to enhance cytokine gene transcription, such as Tat, might be responsible for this effect. The absence of Nef leads to higher IL-2 production upon TCR engagement, suggesting that Nef, in the context of HIV-1 infection, may act as a negative modulator of the IL-2 pathway.

Altogether, these results show that HIV-1 infection impairs the capacity of lymphocytes to form synapses and to transduce early TCR signals in a Nef-dependent manner, whereas downstream signaling pathways leading to IL-2 production are upregulated independently of synapse formation.

Discussion

We provide here fresh insights into the effects of HIV-1 infection on T cell physiology. We show that HIV-1 impairs the formation of the immunological synapse. Conjugation of infected lymphocytes with APCs, as well as clustering of TCRs and Lck, hallmarks of the immunological synapse, are strongly inhibited. Tyrosine phosphorylation patterns are also altered upon infection. Most of these effects are mediated by the viral protein Nef, which profoundly modifies endosomal traffic of Lck and TCR.

Although the presence of Lck in dynamic endosomal vesicles was previously reported (Ehrlich et al., 2002), its relevance in lymphocyte biology remained elusive. It is worth noting that the intracellular trafficking of *src* family kinases in general is poorly characterized. Our results demonstrate that HIV-1 targeted this transport pathway, not only for Lck, but also for TCR, as a means to modulate early lymphocyte responses. This underscores the dynamic importance of endosomal trafficking for subcellular localization, transport to the synapse, and activity of key cellular proteins.

The molecular mechanism by which Nef alters Lck and TCR trafficking is not fully understood. Since Lck interacts with CD4 (Turner et al., 1990), misrouting of Lck could have been due to Nef-induced CD4 downregulation. It is unlikely that this is the case, since we show that Nef induces Lck endosomal accumulation in Jurkat cells lacking CD4. Moreover, the NefLL/AA mutant, which no longer downregulates CD4, induces Lck intracellular accumulation. The fact that Nef and Lck can interact with each other (Baur et al., 1997; Greenway et al., 1996) and that both proteins are found in membrane rafts (Sol-Foulon et al., 2004; Wang et al., 2000), which are continuously endocytosed and recycled (Mayor and Riezman, 2004), could provide an explanation for the alteration of Lck trafficking by Nef. However, this will require further investigation. Regarding TCR trafficking, the mechanism may be even more complex, due to the multiple subunits of this receptor. An interaction between Nef and the TCRζ subunit was reported both for HIV and SIV. However, SIV Nef, but not HIV Nef, downregulates TCR surface expression (Swigut et al., 2003; Xu et al., 1999). Therefore, proteins from human and simian viruses affect TCR trafficking by different ways.

A role for Nef-induced CD28 and CD4 downregulation in the synapse defects reported here is unlikely, since the NefLL/AA mutant, which lost competence to modulate these two receptors, strongly modifies TCR and Lck trafficking and inhibits clustering at the immune synapse.

It is also unlikely that the reported effect of Nef on endosomal trafficking and morphology (Madrid et al., 2005; Sanfridson et al., 1997) was the only cause of misrouting of Lck and TCR. First, Nef affects the routing of Lck, TCR, and TfR in different manners. Endosomal accumulation of Lck and TfR is associated with a reduction of the surface levels of these proteins, which would be consistent with reduced recycling or increased endocytosis. In contrast, TCR surface levels were not reduced in HIV-1-infected cells, but slightly increased, consistent with the inhibition of TCR endocytosis that we report. Second, whereas the inhibition of TfR recycling requires the dileucine motif of Nef (Madrid et al., 2005), misrouting of Lck and TCR are independent of this motif. Therefore, Nef has evolved different strategies to impact the traffic of these three molecules through the endosomal compartment.

The decreased number of T cell-APC conjugates observed upon HIV infection might be due to defects in the initial cell adhesion or in the stability of cell conjugates. T cell-APC adhesion is controlled by multiple proteins, like the integrins LFA-1, ICAM-1, ICAM-3, CD2, CD28, etc., which ensure first cell contact as well as stability of the interaction once antigen recognition has occurred. TCR and coreceptor activation increases avidity of the LFA-1 integrin for its ligands, through an actin-dependent inside-out signaling process (Kinashi, 2005). We did not observe any significant variations of the surface levels of ICAM-1, ICAM-3, CD2, or LFA1 in HIV-1 infected cells, suggesting that initial T cell-APC adhesion was not affected. However, mislocalization of Lck and TCR may lead to impaired inside-out signaling to integrins (Morgan et al., 2001) and, as a consequence, to a lower strength of T cell-APC interactions. Moreover, the effect of Nef on LFA-1 signaling (Witte et al., 2004), or the interaction of Nef with the DOCK2-ELMO complex (Janardhan et al., 2004), a key Rac activator involved in immune synapse formation (Sanui et al., 2003), may also account for some of these effects.

HIV-infected lymphocytes displayed lower levels of tyrosine-phosphorylated proteins at the synapse and an altered pattern of tyrosine phosphorylated proteins. Again, these defects were in large part caused by Nef. However, the normal pattern of tyrosine phosphorylation was not

fully recovered with Δ*nef*, suggesting that other viral proteins may also affect signal transduction. It is unclear why in Δ*nef*-infected cells tyrosine phosphorylation at the synapse was as efficient as in control cells, as judged by immunofluorescence, whereas this was not the case when proteins were analyzed by Western blotting. This is likely due to the different sensitivities of the two assays.

It has been recently reported that Nef-expressing Jurkat cells (in the absence of other viral proteins), when activated with anti-CD3 coated beads, accumulated Nef at this surrogate synapse (Fenard et al., 2005). This resulted in normal, or even increased, TCR clustering. Differences in TCR clustering between this study and ours are likely due to the different TCR stimuli utilized. High-affinity TCR ligation by Abs crosslinks and clusters TCRs by a different mechanism than that induced by Ag or sAg-pulsed APCs. Of note, we observed in HIV-infected cells a polarization of the Nef^+ intracellular compartment to the APC contact site, without any obvious Nef clustering at the immunological synapse (data not shown). This apparent discrepancy with Fenard's study is again likely due to the distinct types of Nef expression (virus versus isolated protein) and cell stimulation and to differences in image resolution that result from the use of beads versus APCs.

Interestingly, we show that late activation events, measured by following IL-2 production, were enhanced in HIV-1-infected cells. Likewise, Fenard et al. also reported an increase in NF-AT and NF-kB activation in cells expressing Nef and activated by anti-CD3-CD28 Abs (Fenard et al., 2005). However, we show that this hyperactivation occurred in cells stimulated with sAg-pulsed APCs, or with activators of PKC and calcineurin (PMA and calcium ionophore). Therefore, enhanced IL-2 production seems not related to synapse formation. Moreover, upon TCR stimulation, IL-2 production was more enhanced with HIVΔ*nef* than with HIVwt. This was not the case with PMA/I, which similarly hyperstimulated Nef^+ and Nef^- HIV-infected cells. It will be worth determining which viral components, besides Nef, affect signal transduction pathways downstream of PKC activation and how these components crosstalk with Nef to modulate the IL-2 production pathway. Therefore, HIV-1 infection interferes with signal transduction pathways at different levels and with different outcomes.

What would be the advantages for HIV to inhibit the formation of the immunological synapse and to manipulate TCR-proximal intracellular signaling pathways, while facilitating later events like IL-2 production? By altering immune synapse formation and the TCR activation cascade, Nef might prevent apoptosis that results from repetitive TCR stimulation. This, together with enhanced IL-2 secretion, might increase the life span of infected cells and facilitate viral spread. This process might also favor the development of quiescent, latently infected, lymphocytes (Williams and Greene, 2005). Nef also impairs various apoptotic signals (Geleziunas et al., 2001; Wolf et al., 2001; Xu et al., 1999). Altogether, these combined effects of Nef may confer a selective advantage for infected lymphocytes that would be favorable for cell survival.

Finally, it is noteworthy that a major route of propagation for HIV (as for other retroviruses such as HTLV-1) may be direct cell-to-cell spread. This mode of transmission involves the formation of virological synapses, which in some aspects are similar to immunological synapses (for a recent review, see Piguet and Satenteau [2004]). Interestingly, while HIV-1 inhibits immunological synapses (as reported here), it promotes the formation of virological synapses (Piguet and Satenteau, 2004). It is tempting to speculate that HIV manages to balance between these two types of cell-to-cell crosstalk to improve its own survival and propagation.

Experimental Procedures

Cells, Viruses, and Infections

The human T cell line Jurkat clone J77cl20, the APC Raji, and the sAg-specific peripheral blood T cell lines derived from healthy donors were previously described (Das et al., 2004). The $CD4^+$ (Jurkat Cl20) and the $CD4^-$ (Jurkat Cl45) were obtained from the parental Jurkat line J77.7 by limiting dilution and were characterized by flow cytometry. Jurkat cells or sAg-specific peripheral blood T cell lines derived from healthy donors were infected with HIV-1 X4-tropic strain NL4.3 (HIVwt) and with NL4.3Δnef (HIVΔ*nef*) as described (Sol-Foulon, JBC 2005). HIV-1 NL4.3 carrying either the HIV-1 SF2 *nef* wt gene or the SF2 *nef*LL/AA mutant were a kind gift of Oliver Fackler. Wt and nef-deleted HIV expressing the GFP marker protein were a kind gift of Frank Kirchhoff. Lentiviral vectors containing the *nef*-wt or the *nef*-G2A genes were used to express Nef, as previously described (Maréchal et al., 1998; Petit et al., 2001; Sol-Foulon et al., 2004).

Antibodies and Immunofluorescence Reagents

The anti-CD3 mAbs, OKT3, and UCHT-1, the anti-TfR mAb OKT9 and fluorescent secondary Abs, were used as described (Das et al., 2004; Roumier et al, 2001). The anti-Lck mAb 3A5 was from Santa Cruz Biotech, California, and the anti-phosphotyrosine mAb 4G10 was from Upstate Biotech Inc., Lake Placid, New York. The anti-HIV-1 Nef mAb MATG020 has been described (Le Gall et al., 1998). The rabbit anti-Gag Ab was a gift from the NIH AIDS Research and Reference Reagent Program. Phycoerithrin-labeled mAbs against CD3 (SK7), CD4 (SK3), CD28 (Leu-28), and IL2-PE and anti-human active Caspase 3-PE were from BD-Pharmingen. Fluorescein-coupled anti-Gag Ab (KC57) was from Beckman-Coulter.

Immunofluorescence and Flow Cytometry

Immunofluorescence and flow cytometry were performed as described (Sol-Foulon et al., 2004).

Immunological Synapse Formation, Confocal Microscopy, and Quantitative Image Analysis

T cell activation, immunofluorescence staining, and confocal microscopy were performed as previously described (Das et al, 2004; Roumier et al., 2001). For detection and further quantification of TCR accumulation at the synapse, conjugates were stained with first and second Abs in the absence of detergent (nonpermeabilizing conditions) to reveal surface receptors only. Then, to detect TCR, Lck, or viral proteins in intracellular compartments, cells were stained in the presence of 0.05 % saponin or 0.1 % Triton X-100 (permeabilizing conditions).

Confocal microscopy was carried out on a Zeiss LSM510 using a 63× objective. Z series of optical sections were performed at 0.2–0.5 μm increments for qualitative analysis. Green and red fluorescence was acquired sequentially to prevent passage of fluoresce from one channel into the other. When required, image deconvolution and 3D reconstruction of images were carried out using Huygens and Osirix software, respectively. Images to quantify were acquired at 2 μm increments with pinholes opened to obtain optical sections of 2 μm thick. Two to three contiguous optical sections per cell conjugate contained all the 3D fluorescence information. Detectors were set to detect an optimal signal below the saturation limits. Image sets to be compared were acquired during the same session and using the same acquisition settings. Fluorescence associated to clusters was quantified using Metamorph software (Universal Imaging, Downingtown, Pennsylvania). After setting a threshold for nonsignificant coefficients, the total gray level of pixels corresponding to

clusters at the synapse, or to intracellular Lck compartment, was measured. The same threshold was used for all the images of a quantification series. For activated T cells, only conjugates displaying TCR clusters were quantified. This type of quantification based on the total fluorescence intensity due to TCR accumulation at the synapse is meant to reflect the total amount of TCRs accumulated at the APC contact site at a given time, independently of their density per surface unit, that would also reflect the local organization in clusters. To estimate Lck accumulation in the intracellular compartment, the ratio between the intensity of fluorescence in the intracellular compartment and the total fluorescence of each cell was calculated. To estimate the amount of TCRs accumulated in the pericentriolar compartment, a region was defined in that region and used in noninfected as well as infected cells. The ratio between the intensity of fluorescence in the intracellular compartment and the total fluorescence of each cell was calculated. Values were represented as dot plots, with each dot representing the value of an individual cell. Statistical analyses were carried out by the nonparametrical Mann-Whitney test using Statview or PRISM softwares. A difference between values was considered significant when a $p < 0.05$ was obtained.

T Cell Activation and Phophotyrosine Analyses

Activation and phosphotyrosine analysis was performed as described (Michel et al., 2001; Niedergang et al., 1998). Briefly, Jurkat cells uninfected or infected with HIVwt or HIVΔ*nef* were used at the peak of infection, as assessed by intracellular Gag staining, and before the occurrence of major cytopathic effects. Cells (3×10^6) were stimulated with Raji cells (10^6) prepulsed with 10 μg/ml *Staphylococcus* enterotoxin E (SEE) sAg for 2 min or 15 min. Cells were centrifuged and lysed, and whole lysates were analyzed with anti-phosphotyrosine mAbs, anti Lck, and anti-Nef. Part of the lysates was immunoprecipitated with anti-Lck mAb and further analyzed by electrophoresis and Western blotting using anti-phosphotyrosine mAb and anti-Lck.

IL-2 Production

Jurkat cells, uninfected or infected with HIV-1 wt or Δ*nef*, were used before the peak of infection (20%–50% intracellular Gag^+). Then, 3×10^5 cells were left untreated or stimulated for 4 hr with phorbol-12-myristate-13-acetate (PMA) (25 ng/ml) + calcium ionophore A23187 (1 μg/ml) or with 10^5 Raji cells prepulsed with SEE (0.1 μg/ml). Cells were then fixed with 2% PFA for 20 min, permeabilized for 10 min, and stained in permeabilisation buffer with anti-human IL2-PE and anti-Gag-FITC for 30–45 min. After washes with PBS/1% BSA, samples were analyzed on a FACS Calibur flow cytometer (Becton Dickinson).

Supplemental Data

Supplemental Data include six figures and two movies and can be found with this article online at http://www.immunity.com/cgi/content/full/24/5/■ ■ ■/DC1/.

Acknowledgments

This work was supported by grants from La Ligue Contre le Cancer-Comité de Paris, l'Agence Nationale de Recherche sur le SIDA, Sidaction, the Centre National de la Recherche Scientifique, the European Community, and the Institut Pasteur. F.B. has been supported by a fellowship from the European Community and by a Bourse Roux from Institut Pasteur. The technical assistance of A. Dujeancourt, V. Malardé, F. Porrot, and C. Trouillet is thankfully acknowledged. We thank P. Roux, E. Perret, and M. Marchand from the Plate Forme d'Imagerie Dynamique (PFID) at the Institut Pasteur for expert technical assistance with microscopy imaging. We thank Oliver T. Fackler and Frank Kirchhoff for the kind gift of HIV proviruses and the National Institutes of Health AIDS Research and Reference reagent program for providing reagents. None of the authors of this work have a financial interest related to this work.

Received: August 1, 2005
Revised: February 8, 2006
Accepted: February 27, 2006
Published: May 23, 2006

References

Baur, A.S., Sass, G., Laffert, B., Willbold, D., Cheng-Mayer, C., and Peterlin, B.M. (1997). The N terminus of Nef from HIV-1/SIV associates with a protein complex containing Lck and a serine kinase. Immunity *6*, 283–291.

Bonello, G., Blanchard, N., Montoya, M.C., Aguado, E., Langlet, C., He, H.T., Nunez-Cruz, S., Malissen, M., Sanchez-Madrid, F., Olive, D., et al. (2003). Dynamic recruitment of the adaptor protein LAT: LAT exists in two distinct intracellular pools and controls its own recruitment. J. Cell Sci. *117*, 1009–1016.

Bunnell, S.C., Hong, D.I., Kardon, J.R., Yamazaki, T., McGlade, C.J., Barr, V.A., and Samelson, L.E. (2002). T cell receptor ligation induces the formation of dynamically regulated signaling assemblies. J. Cell Biol. *158*, 1263–1275.

Collette, Y., Dutartre, H., Benziane, A., Ramos, M., Benarous, R., Harris, M., and Olive, D. (1996). Physical and functional interaction of Nef with Lck. HIV-1 Nef-induced T cell signaling defects. J. Biol. Chem. *271*, 6333–6341.

Craig, H.M., Pandori, M.W., and Guatelli, J.C. (1998). Interaction of HIV-1 Nef with the cellular dileucine-based sorting pathway is required for CD4 down-regulation and optimal viral infectivity. Proc. Natl. Acad. Sci. USA *95*, 11229–11234.

Das, S.R., and Jameel, S. (2005). Biology of the HIV Nef protein. Indian J. Med. Res. *121*, 315–332.

Das, V., Nal, B., Dujeancourt, A., Thoulouze, M.I., Galli, T., Roux, P., Dautry-Varsat, A., and Alcover, A. (2004). Activation-induced polarized recycling targets T cell receptors to the immunological synapse. Involvement of SNARE complexes. Immunity *20*, 577–588.

Dietrich, J., Menné, C., Lauritsen, J.P.H., von Essen, M., Rasmussen, A.B., Odum, N., and Geisler, C. (2002). Ligand-induced TCR down-regulation is not dependent on constitutive TCR cycling. J. Immunol. *168*, 5434–5440.

Egen, J.G., and Allison, J.P. (2002). Cytotoxic T lymphocyte antigen-4 accumulation in the immunological synapse is regulated by TCR signal strength. Immunity *16*, 23–35.

Ehrlich, L.I.R., Ebert, P.J.R., Krummel, M.F., Weiss, A., and Davis, M.M. (2002). Dynamics pf p56lck translocation to the T cell immunological synapse following agonist and antagonist stimulation. Immunity *17*, 809–822.

Fenard, D., Yonemoto, W., de Noronha, C., Cavrois, M., Williams, S.A., and Greene, W.C. (2005). Nef is physically recruited into the immunological synapse and potentiates T cell activation early after TCR engagment. J. Immunol. *175*, 6050–6057.

Geleziunas, R., Xu, W., Takeda, K., Ichijo, H., and Green, W.C. (2001). HIV-1 Nef inhibits ASK1-dependent death signalling providing a potential mechanism for protecting the infected host cell. Nature *410*, 834–838.

Grakoui, A., Bromley, S.K., Sumen, C., Davis, M.M., Shaw, A.S., Allen, P.M., and Dustin, M.L. (1999). The immunological synapse: a molecular machine controling T cell activation. Science *285*, 221–227.

Greenway, A., Azad, A., Mills, J., and McPhee, D.A. (1996). Human immunodeficiency virus type 1 Nef binds directly to Lck and mitogen-activated protein kinase, inhibiting kinase activity. J. Virol. *70*, 6701–6708.

Greenway, A.L., Holloway, G., McPhee, D.A., Ellis, P., Cornall, A., and Lidman, M. (2003). HIV-1 Nef control of cell signalling molecules: multiple strategies to promote virus replication. J. Biosci. *28*, 323–335.

Holdorf, A.D., Lee, K.H., Burack, W.R., Allen, P.M., and Shaw, A.S. (2002). Regulation of Lck activity by CD4 and CD28 in the immunological synapse. Nat. Immunol. *3*, 259–264.

Huppa, J.B., Gleimer, M., Sumen, C., and Davis, M.M. (2003). Continuous T cell receptor signaling required for synapse maintenance and full effector potential. Nat. Immunol. *8*, 749–755.

Irvine, D.J., Purbhoo, M.A., Krogsgaard, M., and Davis, D.M. (2002). Direct observation of ligand recognition by T cells. Nature *419*, 845–849.

Janardhan, A., Swigut, T., Hill, B., Myers, M.P., and Skowronski, J. (2004). HIV-1 Nef binds to the DOCK2-ELMO complex to activate Rac and inhibit lymphocyte chemotaxis. PLoS Biol. *2*, 65–76.

Kinashi, T. (2005). Intracellular signalling controlling integrin activation in lymphocytes. Nat. Rev. Immunol. *5*, 546–559.

Krogsgaard, M., Huppa, J.B., Purbhoo, M.A., and Davis, M.M. (2003). Linking molecular events in T-cell activation and synapse formation. Semin. Immunol. *15*, 307–315.

Krummel, M.F., Sjaastad, M.D., Wülfing, C., and Davis, M.M. (2000). Differential clustering of CD4 and CD3ζ during T cell recognition. Science *289*, 1349–1352.

Lee, K.H., Holdorf, A.D., Dustin, M.L., Chan, A.C., Allen, P., and Shaw, A.S. (2002). T cell receptor signaling precedes immunological synapse formation. Science *295*, 1539–1542.

Lee, K.H., Dinner, A.R., Tu, C., Campi, G., Raychaudhuri, S., Varma, R., Sims, T.N., Burack, W.R., Wu, H., Wang, J., et al. (2003). The immunological synapse balances T cell receptor signaling and degradation. Science *302*, 1218–1222.

LeGall, S., Erdtmann, L., Benichou, S., Berlioz-Torrent, C., Liu, L.X., Benarous, R., Heard, J.M., and Schwartz, O. (1998). Nef interacts with μ subunits of clathrin adaptor complexes and reveals a cryptic sorting signal in MHC-I molecules. Immunity *8*, 483–495.

Ley, S.C., Marsh, M., Bebbington, C.R., Proudfoot, K., and Jordan, P. (1994). Distinct intracellular localization of Lck and Fyn protein tyrosine kinases in human T lymphocytes. J. Cell Biol. *125*, 639–649.

Li, Q.J., Dinner, A.R., Qi, S., Irvine, D.J., Huppa, J.B., Davis, M.M., and Chakaborty, A.K. (2004). CD4 enhances T cell sensitivity to antigen by coodinating Lck accumulation at the immunological synapse. Nat. Immunol. *5*, 791–799.

Madrid, R., Janvier, K., Hitchin, D., Day, J., Coleman, S., Noviello, C., Bouchet, J., Benmerah, A., Gautelli, J., and Benichou, S. (2005). Nef-induced alteration of the early/recycling endosomal compartment correlates with enhancement of HIV-1 infectivity. J. Biol. Chem. *280*, 5032–5044.

Maréchal, V., Clavel, F., Heard, J.M., and Schwartz, O. (1998). Free in PMC cytosolic Gag p24 as an index of productive entry of human immunodeficiency virus type 1. J. Virol. *72*, 2208–2212.

Mayor, S., and Riezman, H. (2004). Sorting GPI-anchor proteins. Nat. Rev. Mol. Cell Biol. *5*, 110–120.

Michel, F., Attal-Bonnefoy, G., Mangino, G., Mise-Omata, S., and Acuto, O. (2001). CD28 as a molecular amplifier extending TCR ligation and signaling capabilities. Immunity *15*, 935–945.

Monks, C.R.F., Freiberg, B.A., Kupfer, H., Sciaky, N., and Kupfer, A. (1998). Three-dimensional segregation of supramolecular activation clusters in T cells. Nature *395*, 82–86.

Morgan, M.M., Labno, C.M., Van Seventer, G.A., Denny, M.F., Straus, D.B., and Burkhardt, J.K. (2001). Superantigen-induced T cell:B cell conjugation is mediated by LFA-1 and requires signaling through Lck, but not ZAP-70. J. Immunol. *167*, 5708–5718.

Niedergang, F., Hémar, A., Hewitt, C.R.A., Owen, M.J., Dautry-Varsat, A., and Alcover, A. (1995). The *Staphylococcus aureus* enterotoxin B superantigen induces specific T cell receptor down-regulation by increasing its internalization. J. Biol. Chem. *270*, 12839–12845.

Niedergang, F., San José, E., Rubin, B., Alarcón, B., Dautry-Varsat, A., and Alcover, A. (1997). Differential cytosolic tail dependence and intracellular fate of T cell receptors internalized upon activation with superantigen or phorbol ester. Res. Immunol. *148*, 225–239.

Niedergang, F., Dautry-Varsat, A., and Alcover, A. (1998). Cooperative activation of TCRs by enterotoxin superantigens. J. Immunol. *161*, 6054–6058.

Petit, C., Buseyne, F., Boccaccio, C., Abastado, J.P., Heard, J.M., and Schwartz, O. (2001). Nef is required for efficient HIV-1 replication in cocultures of dendritic cells and lymphocytes. Virology *286*, 225–236.

Piguet, V., and Satenteau, Q. (2004). Dangerous liaisons at the virological synapse. J. Clin. Invest. *114*, 605–610.

Piguet, V., Schwartz, O., Le Gall, S., and Trono, D. (1999). The downregulation of CD4 and MHC-1 by primate lentiviruses: a paradigm for the modulation of cell surface receptors. Immunol Rev. *168*, 51–63.

Roumier, A., Olivo-Marin, J.C., Arpin, M., Michel, F., Martin, M., Mangeat, P., Acuto, O., Dautry-Varsat, A., and Alcover, A. (2001). The membrane-microfilament linker ezrin is involved in the formation of the immunological synapse and in T cell activation. Immunity *15*, 715–728.

Salghetti, S., Mariani, R., and Skowronski, J. (1995). Human immunodeficiency virus type 1 Nef and p56lck protein-tyrosine kinase interact with a common element in CD4 cytoplasmic tail. Proc. Natl. Acad. Sci. USA *92*, 349–353.

Sanfridson, A., Hester, S., and Doyle, C. (1997). Nef proteins encoded by human and simian immunodeficiency viruses induce the accumulation of endosomes and lysosomes in human T cells. Proc. Natl. Acad. Sci. USA *94*, 873–878.

Sanui, T., Inayoshi, A., Noda, M., Iwata, E., Oike, M., Sasazuki, T., and Fukui, Y. (2003). DOCK2 is essential for antigen-induced translocation of TCR and lipid rafts but not PKC-θ and LFA-1, in T cells. Immunity *19*, 119–129.

Sechi, A.S., and Wehland, J. (2004). Interplay between TCR signalling and actin cytoskeleton dynamics. Trends Immunol. *25*, 257–265.

Simmons, A., Aluvihare, V., and McMichael, A. (2001). Nef triggers a transcriptional program in T cells imitating single-signal T cell activation and inducing HIV virulence mediators. Immunity *14*, 763–777.

Sol-Foulon, N., Esnault, C., Percherancier, Y., Porrot, F., Metais-Cunha, P., Bachelerie, F., and Schwartz, O. (2004). The effects of HIV-1 Nef on CD4 surface expression and viral infectivity in lymphoid cells are independent of rafts. J. Biol. Chem. *279*, 31398–31408.

Swigut, T., Greenberg, M., and Skowronski, J. (2003). Cooperative interactions of simian immunodeficiency virus Nef, AP2, and CD3-ζ mediate the selective induction of T-cell receptor-CD3 endocytosis. J. Virol. *77*, 8116–8126.

Turner, J.M., Brodsky, M.H., Irving, B.A., Levin, S.D., Perlmutter, R.M., and Littman, D.R. (1990). Interaction of the unique N-terminal region of tyrosine kinase p56lck with cytoplasmic domains of CD4 and CD8 is mediated by cystein motifs. Cell *60*, 755–765.

Vidal, K., Daniel, C., Hill, M., Littman, D.R., and Allen, P.M. (1999). Differential requirements for CD4 in TCR-ligand interactions. J. Immunol. *163*, 4811–4818.

Wang, J.K., Kiyosawa, E., Verdin, E., and Trono, D. (2000). The Nef protein of HIV-1 associates with rafts and primes T cells for activation. Proc. Natl. Acad. Sci. USA *97*, 394–399.

Williams, S.A.F., and Greene, W.C. (2005). Host factors regulating post-integration latency of HIV. Trends Microbiol. *13*, 137–139.

Witte, V., Laffert, B., Rosorius, O., Lischka, P., Blume, K., Galler, G., Stilper, A., Willbold, D., D'Aloja, P., Sixt, M., et al. (2004). HIV-1 Nef mimics an integrin receptor signal that recruits the polycomb group protein Eed to the plasma membrane. Mol. Cell *13*, 179–190.

Wolf, D., Witte, V., Laffert, B., Blume, K., Stromer, E., Trapp, S., d'Aloja, P., Schurmann, A., and Baur, A.S. (2001). Nef-associated PAK and PI3-kinase stimulate Akt-independent Bad phosphorylation to induce anti-apoptotic signals. Nat. Med. *7*, 1217–1224.

Wu, Y., and Marsh, J.W. (2001). Selective transcription and modulation of resting T cell activity by preintegrated HIV DNA. Science *293*, 1503–1506.

Wülfing, C., and Davis, M.M. (1998). A receptor/cytoskeletal movement triggered by costimulation during T cell activation. Science *282*, 2266–2269.

Xu, X.N., Laffert, B., Screaton, G.R., Kraft, M., Wolf, D., Kolanus, W., Mongkolsapay, J., McMichael, A., and Baur, A.S. (1999). Induction of Fas ligand expression by HIV involves the interaction of Nef with the T cell receptor ζ chain. J. Exp. Med. *189*, 1489–1496.